Title
Increased Modularity of Resting State Networks Supports Improved Narrative Production in Aphasia Recovery

Journal
Brain Connectivity, 6(7)

ISSN
2158-0014

Authors
Duncan, E Susan
Small, Steven L

Publication Date
2016-09-01

DOI
10.1089/brain.2016.0437

Peer reviewed

BRAIN CONNECTIVITY
Volume 6, Number 7, 2016

DOI: 10.1089/brain.2016.0437

Increased Modularity of Resting State Networks Supports Improved Narrative Production in Aphasia Recovery

E. Susan Duncan[1] and Steven L. Small[2]

Abstract

The networks that emerge in the analysis of resting state functional magnetic resonance imaging (rsfMRI) data are believed to reflect the intrinsic organization of the brain. One key property of such complex biological networks is modularity, a measure of community structure. This topological characteristic changes in neurological disease and recovery. Nineteen subjects with language disorders after stroke (aphasia) underwent neuroimaging and behavioral assessment at multiple time points before (baseline) and after an imitation-based therapy. Language was assessed with a narrative production task. Group independent component analysis was performed on the rsfMRI data to identify resting state networks (RSNs). For each participant and each rsfMRI acquisition, we constructed a graph comprising all RSNs. We assigned nodal community based on a region's RSN membership, calculated the modularity score, and then correlated changes in modularity and therapeutic gains on the narrative task. We repeated this comparison controlling for pretherapy performance and using a community structure not based on RSN membership. Increased RSN modularity was positively correlated with improvement on the narrative task immediately post-therapy. This finding remained significant when controlling for pretherapy performance. There were no significant findings for network modularity and behavior when nodal community was assigned without consideration of RSN membership. We interpret these findings as support for the adaptive role of network segregation in behavioral improvement in aphasia therapy. This has important clinical implications for the targeting of noninvasive brain stimulation in poststroke remediation and suggests potential for further insight into the processes underlying such changes through computational modeling.

Keywords: aphasia; functional neuroimaging; graph theory; network analysis; rehabilitation; resting state; speech-language pathology; stroke

Introduction

Graph theoretic approaches provide simplified metrics to characterize complex networks. By defining regions as nodes and the (functional or structural) connections between them as edges, the brain can be modeled as a graph and analyzed through the pairwise relationships among its component parts (Rubinov and Sporns, 2010). As measured by resting state functional magnetic resonance imaging (rsfMRI), our brains demonstrate the same types of topological properties found in other complex networks across various systems (Bullmore and Sporns, 2009).

Modularity is one key organizational principle found in social and biological systems (Girvan and Newman, 2002), including the human brain. To characterize the modularity of a network, individual nodes are first assigned to discrete communities by various methods. The modularity value of the network quantifies how many of the edges connected to a given node are also connected to another node within the same community, compared to if those edges had been distributed randomly (Newman and Girvan, 2004). Thus, modularity is essentially an index of how cleanly a network can be subdivided with a given partition, with higher values indicating more distinct subnetworks or a greater level of segregation.

Figure 1 shows two different graphs that share many network characteristics. Each has 34 nodes. They share a similar number of edges connecting those nodes (Fig. 1A = 81, B = 78). They also share a similar degree distribution, with each node having, on average, just fewer than five connections to other nodes (Fig. 1A = 4.76, B = 4.59). Each graph has been separated into five communities, indicated by node color, as this was determined to be the optimal number of communities for maximizing modularity for each of these networks individually. However, the communities in Figure 1A overlap and

Departments of [1]Cognitive Sciences & Neurology and [2]Neurology, Neurobiology & Behavior, Cognitive Sciences, University of California, Irvine, Irvine, California.

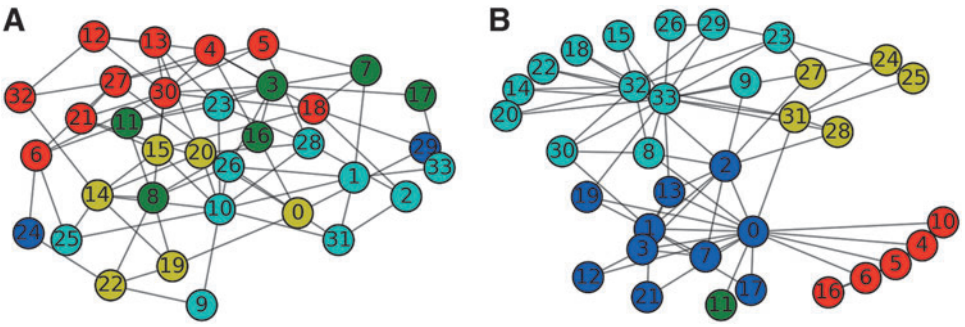

FIG. 1. Visual depiction of two graphs. **(A, B)** share similar network properties, including number of nodes, edges, communities, and average degree, yet the modularity of **(B)** (0.41) is much higher compared with **(A)** (0.27). **(A)** is a random network; **(B)** depicts data from a social organization (Zachary, 1977). Color images available online at www.liebertpub.com/brain

share many edges among them, whereas the communities in Figure 1B are more discrete, and their modularity scores reflect this difference (0.27 and 0.41, respectively). This major difference in their organization is not surprising as the graph in Figure 1A is a random construction, whereas the graph in Figure 1B represents data from a social network (Zachary, 1977).

As modularity is a basic characteristic of complex networks under normal circumstances, it might be expected that a disruption to that network would result in a decrease in its modularity. In the brain, deprivation of blood flow results in changes in both cognitive function and functional connectivity and modularity as assessed by rsfMRI. For patients with unilateral carotid stenosis, modularity is negatively correlated with performance on neuropsychological tasks, including the Mini-Mental Status Examination and measures of reading and memory (Chang et al., 2016), and positively correlated with better postoperative cognitive outcomes (Soman et al., 2016). Focal lesions are also found to reduce measures of modularity (Gratton et al., 2012).

In healthy adults, higher modularity is associated with better working memory performance, a finding thought to reflect efficient organization and transmission of information throughout the brain (Stevens et al., 2012). It may, therefore, be unsurprising that measures of modularity are decreased in patients with Alzheimer disease (AD). This is also true for cognitively intact individuals demonstrating pre-clinical biomarker pathology suggestive of AD (Brier et al., 2014) compared to controls without such pathology. However, even in healthy aging, brain changes are associated with alteration in its modular organization. Whole brain modularity declines with aging across the life span (Onoda and Yamaguchi, 2013), including when examining the modularity of intrinsic resting state networks (RSNs) exclusively (Song et al., 2014).

In a recent investigation of changes in dynamic functional network connectivity in patients with aphasia, we investigated the amount of time spent by each participant in one of the small number of states determined by clustering the dynamic network correlations (E.S. Duncan and S.L. Small, submitted). We found that the amount of time spent in one of these states—a state characterized by minimal correlations among RSNs—was associated with improvement in narrative production. We interpreted these findings as evidence for an association between greater functional segregation and better performance, as previously demonstrated in healthy aging (Chan et al., 2014) and Parkinson's disease (Tinaz et al., 2016). They are also consistent with the finding that diffuse patterns of activation are replaced by more focal, and presumably efficient, organization as behavior improves, as has been found in motor learning (Milton et al., 2007), as well as poststroke motor (Ward et al., 2003) and language (Abel et al., 2015) rehabilitation.

In the present study, we examine the hypothesis that assigning community structure based on membership in well-established RSNs will result in changes in modularity that are positively correlated with behavioral changes in narrative production, as found in dynamic functional connectivity. Such findings would support the notion that successful therapy leads to increased network segregation and would provide insight into the mechanism underlying behavioral improvement following treatment. It would also lead to discovery of possible targets for focal intervention.

Materials and Methods

Participants

Nineteen native English speakers with chronic aphasia secondary to ischemic stroke participated in a larger study of intensive, imitation-based aphasia therapy (Duncan et al., 2016; Lee et al., 2010). Fourteen subjects were selected from that superset based on participation in three baseline rsfMRI scans before the initiation of therapy. Two additional subjects were excluded due to excessive motion during scanning (see rsfMRI Preprocessing section for details). The remaining group included in this analysis consisted of 12 individuals (3 female; 25%) ages 31–70 years (mean = 52.08; SD = 11.75) who had sustained a single stroke 7–124 months before enrollment (mean = 40.33; SD 42.55).

The study was approved by the Institutional Review Boards of the University of Chicago and the University of California, Irvine. Consent was obtained according to the Declaration of Helsinki.

Behavioral measures

A full description of the Cinderella task and associated behavioral results were reported previously (E.S. Duncan and S.L. Small, under review). Participants were recorded telling a narrative (Cinderella) (Saffran et al., 1989) four times over an 18-week span (weeks −6, 0, 6, 12) during which the middle 6 weeks (weeks 0–6) consisted of the Intensive Mouth Imitation and Talking for Aphasia Therapeutic Effect (IMITATE) therapy. The recorded narratives were scored for number of correct information units (CIUs) produced. Words were counted as CIUs if they were novel, intelligible, and appropriate to the context. Figure 2 depicts the study design. One subject (10) missed the fourth behavioral evaluation.

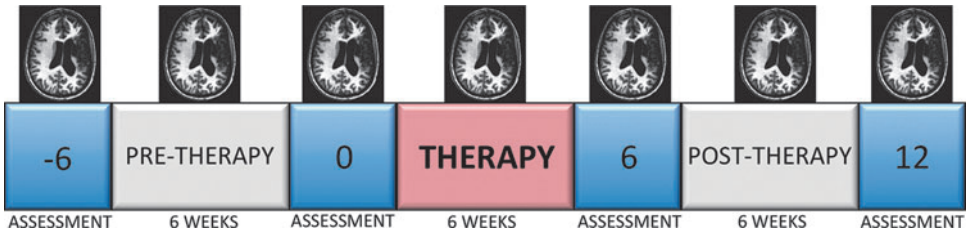

FIG. 2. Study design. Total study duration was 18 weeks. Six week baseline preceded a 6 week course of therapy, which was followed by a 6 week maintenance interval. Numbers indicate weeks at which behavioral assessment was performed. Magnetic resonance images indicate time points at which neuroimaging was acquired. Color images available online at www.liebertpub.com/brain

Neuroimaging measures

Acquisition. MRI was acquired at three baseline time points before 6 weeks of therapy (weeks −6, −3, 0) and at up to three time points following the end of treatment (weeks 6, 9, 12). Figure 2 depicts the study design. Images were acquired on a 3T Siemens Trio MRI scanner (Siemens Medical Solutions USA, Inc., Malvern, PA) at the Northwestern University. High resolution structural images were acquired using a T1-MPRAGE sequence with TR = 2300 msec, TE = 3.36 msec, TI = 900 msec, flip angle = 9°, and 1 mm isotropic voxel size. rsfMRI images were acquired using an EPI sequence with TR = 1500 msec, TE = 20 msec, flip angle = 71°, FOV = 220 × 220 mm^2, matrix size = 64 × 64, 29 axial slices with 4 mm thickness (1 mm gap), and inplane voxel size of 3.75 × 3.75 mm. During 5 min of scanning, 200 volumes were acquired.

rsfMRI preprocessing. rsfMRI preprocessing consisted of discarding the first four volumes, slice timing correction, despiking, and registration performed using Analysis of Functional NeuroImages (AFNI) (Cox, 1996) and FMRIB Software Library (FSL) (Smith et al., 2004). The AFNI function 3dDeconvolve was used to regress out signals of no interest (from white matter, ventricles, and lesion), as well as motion and polynomial (linear and quadratic) trends. If a volume had >3 mm displacement from the volume to which it was being registered, both that volume and the following one were censored and not included in the regression. A scan needed to have ≥55% of volumes uncensored (108) to be included in the analysis. These cleaned time series were then band-pass filtered (0.01–0.1 Hz) to identify the low frequency fluctuations of interest. As some participants missed or had excessive motion during one or two scanning sessions, a total of 76 scans were included in this analysis (rather than 12 subjects × 7 scans = 84).

Anatomical preprocessing. Lesion masks drawn on the high-resolution structural scans were used to perform a Virtual Brain Transplant (Solodkin et al., 2010) to facilitate reconstruction of each participant's cortical surface with FreeSurfer (Fischl, 2012), brain parcellation into 463 regions (Hagmann et al., 2008), and the creation of a common template. Each participant's preprocessed and band-pass filtered rsfMRI was registered to the common template to permit group analysis.

Independent component analysis. Spatial independent component analysis (ICA) was performed using the Group ICA of fMRI Toolbox (GIFT) (Calhoun, 2004). In a preprocessing step before ICA, the time series underwent mean centering followed by whitening and dimension reduction using subject-specific principal component analysis to extract the first 20 eigenvectors (low-order Gaussian features). Group ICA using the Infomax algorithm then identified 20 independent higher-order non-Gaussian features of the reduced data. ICA was repeated 10 times with random initiation and bootstrapping to ensure the stability of the identified components (ICASSO) (Himberg et al., 2004).

Graph construction. Eight of the 20 identified components were selected as components of interest (E.S. Duncan and S.L. Small, submitted) that did not overlap with regions of known vascular, motion, and susceptibility artifacts and that were consistent with RSNs previously identified in the literature (Damoiseaux et al., 2006; Lee et al., 2012). We took the inverse of the transformation that registered individual scans to the group template and applied it to these eight RSNs to bring them from standard space into the native space in which the rsfMRI data were acquired. We then took the intersection of anatomical regions for each of the RSNs for all participants, using the parcellation scheme applied during preprocessing of the anatomical volume (Hagmann et al., 2008). Each RSN included between 24 and 40 regions, for a total of 230 regions among the eight RSNs. After identifying the peak voxel for each region included in any one of the eight RSNs for each scan, we mean centered the time series and constructed a joint covariance matrix for all time series in all 230 regions. We induced sparsity in these matrices using the graphical lasso (Friedman et al., 2008) as implemented in R (Friedman et al., 2014), and we used the resulting inverse covariance matrix to construct a graph for each scan using NetworkX (Hagberg et al., 2004). In these graphs, each region is a node, and the edges are weighted by the strengths of the functional connectivity (covariance).

Modularity. Processing of the functional connectivity graphs included first removing all negative edges and then binarizing the remaining positive edges. We assigned each node of these resulting graphs to a module based on its membership in one of the original eight RSNs and then computed a modularity value (Q) for each scan through use of the NetworkX community modularity function (Hagberg et al., 2008) based on a well-established metric (Newman and Girvan, 2004).

To control for graphs simply changing in modularity without any consideration of RSNs, nodes were also assigned to modules based on a separate partition determined through

application of a community detection algorithm using the Louvain method (Blondel et al., 2008), with a separate modularity score calculated.

Correlation of modularity and behavior

Differences in modularity (Q) were correlated with differences in number of CIUs produced before and after therapy. Pretherapy modularity was calculated as the average Q of the three baseline scans (weeks −6, −3, 0). Post-therapy modularity was calculated as the average Q for the scans (from 1 to 3 total) acquired after therapy (weeks 6, 9, 12). The pretherapy CIU score was defined as the average number of CIUs for the two pretherapy assessments. The post-therapy CIU score was averaged across the two post-therapy testing sessions (week 6, 12). Four comparisons were made for the changes that occurred in behavior and functional RSN modularity as follows: post-therapy versus pretherapy, week 6 versus pretherapy, week 12 versus pretherapy, and week 12 versus week 6. These correlations were corrected for the three independent comparisons ($\alpha = 0.05/3$).

Significant comparisons were repeated twice: (1) using partial correlations controlling for pretherapy CIU production and (2) using a separate community assignment partition (see Modularity section) to control for changes in modularity unrelated to RSNs.

A repeated measure analysis of variance (ANOVA) was used to compare baseline Q values to ensure that RSN modularity did not significantly differ among pretherapy scans.

Results

There was a positive correlation between change in CIUs and change in RSN modularity comparing pre- and post-therapy measures ($r = +0.687$; $p = 0.014$) and comparing week 6 measures to baseline ($r = +0.760$; $p = 0.011$). Figure 3 shows these relationships. Neither the correlation of week 12 with baseline ($r = +0.549$; $p = 0.100$) nor week 12 with week 6 ($r = +0.237$; $p = 0.572$) was significant. Reduced power due to missed scans (leaving 8 or 10 subjects) may have played a role in the failure of these comparisons to reach significance.

Controlling for pretherapy CIU production, the pre- versus post-therapy partial correlation ($r = +0.758$; $p = 0.007$) and the week 6 partial correlation ($r = +0.676$; $p = 0.046$) remained significant at $\alpha = 0.05$. There were no significant results for the control comparisons, in which nodes were assigned to communities based on an independent algorithm, rather than RSN membership ($|r| < 0.484$; $p > 0.110$).

An ANOVA comparing baseline modularity indicated no significant differences among the three pretherapy sessions ($p = 0.273$).

Discussion

The present study provides confirmatory evidence for the hypothesis that individuals demonstrating behavioral improvement in narrative production following imitation-based aphasia therapy demonstrate increased segregation among functional networks. We interpret this to mean that increased functional segregation supports a better ability to communicate a narrative. The present finding of improved behavioral performance and increased network modularity when a node's community is assigned based on RSN association also supports the notion of an adaptive role for increased segregation.

Decreased modularity is associated with functional deficits in a variety of disorders, including AD and carotid stenosis (Brier et al., 2014; Chang et al., 2016). However, it should be noted that higher modularity is also associated with decreased performance in some studies. Increased modularity is found in patients with multiple sclerosis (Muthuraman et al., 2016), for whom it is negatively correlated with working memory (Gamboa et al., 2014). In Parkinson's disease, results have been mixed (Baggio et al., 2014; Ma et al., 2016). These findings may indicate that, as with essentially all biological properties, there is an inverse U-shaped curve associated with the modularity of functional brain connectivity. If the modular organization of the brain is either too weak or too strong, the behavior of the organism is maladaptive.

However, for the present findings, it is believed that there is explanatory power associated with the observed changes in brain connectivity. Studies of healthy controls indicate that modularity decreases when task-based fMRI is compared to rsfMRI (Diet al., 2013), as well as when task demands increase (Vatansever et al., 2015). Given that individuals with aphasia demonstrate deficits in cognitive domains outside language (Murray, 2012), the observed recovery in narrative production may be associated not only with language-specific improvement but also with cognitive benefit, resulting in better behavioral performance, as well as decreasing required effort. In addition, connectivity changes in the language system secondary to stroke can ripple throughout other brain subnetworks not directly related to language (Warren et al., 2009), causing connectivity changes both within and between modules.

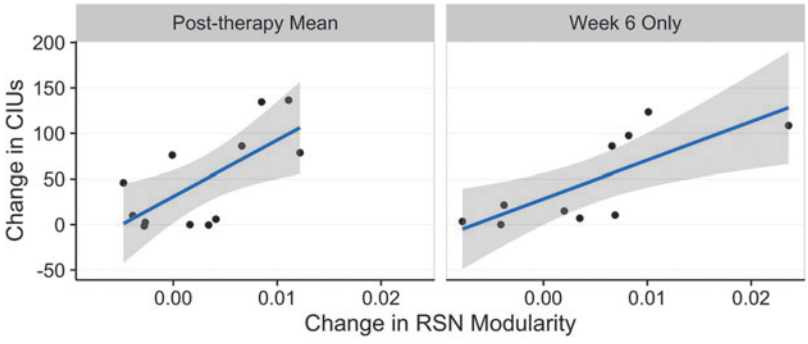

FIG. 3. Correlations between changes in CIU production and RSN modularity. Significant positive correlations for post- compared to pretherapy measures (left) and for immediate post-therapy (week 6) compared to pretherapy. CIU, correct information units; RSN, resting state network. Color images available online at www.liebertpub.com/brain

While graph theoretical analyses are generally underutilized in the study of aphasia and other sequelae of stroke, a few prior studies use such methods to illuminate behavioral changes occurring following brain injury and therapy. In aphasia, local increases in network connectivity are found in bilateral angular gyrus and left pars triangularis, part of Broca's area, in individuals demonstrating benefit from a word finding treatment (Sandberg et al., 2015). Aphasia severity is associated with disruption of regions serving as connector hubs in the language network and a global reduction in the rich club coefficient (Gleichgerrcht et al., 2015), a measure of the tendency for highly connected nodes to be highly interconnected with each other. Patients with the semantic variant of primary progressive aphasia demonstrate lower global efficiency, or more remote functional connections, compared to controls (Agosta et al., 2014), as do those with post-stroke motor deficits (Falcon et al., 2015). These findings suggest, similar to those of the present investigation, that the ability to effectively manage and transmit information throughout the brain is compromised following stroke, that these changes underlie behavioral impairment, and that the restoration of these properties may facilitate functional gains.

Conclusion

The restoration of normal network topology in the brain is a challenge that remains despite these collected findings of disturbance. Targeted stimulation or inhibition of nodes and modules demonstrating deviant patterns of connectivity, with the aim of reinstating network balance, can currently be explored transcranially through magnetic or direct current stimulation. Future insight into the neural mechanisms through which these changes occur may come from ''build to understand'' approaches, such as modeling with The Virtual Brain (Falcon et al., 2015; Jirsa et al., 2010). Better understanding of the biological underpinnings of network disruption and reorganization will stimulate more informed and effective interventions that, in turn, will promote greater recovery.

Acknowledgments

This work was supported by the National Institute of Deafness and other Communication Disorders (NIDCD) of the National Institutes of Health (NIH) under grants R01-DC007488 and R33-DC008638; the James S. McDonnell Foundation under a grant to the Brain Network Recovery Group (A.R. McIntosh, PI); and Mr. William Rosing, Esq. All speech and language evaluations were coordinated by Dr. Leora Cherney at the Rehabilitation Institute of Chicago (RIC) and performed by her staff at RIC. The research staff at the University of Chicago included Blythe Buchholz and Robert Fowler, who helped coordinate the project, and Dan Rodney, who authored the IMITATE software. Dr. Ana Solodkin supervised the drawing of lesion masks. The support of these individuals is gratefully acknowledged, as are the patients and families who generously participated in this research.

Author Disclosure Statement

No competing financial interests exist.

References

Abel S, Weiller C, Huber W, Willmes K, Specht K. 2015. Therapy-induced brain reorganization patterns in aphasia. Brain 138:1097–1112.

Agosta F, Galantucci S, Valsasina P, Canu E, Meani A, Marcone A, et al. 2014. Disrupted brain connectome in semantic variant of primary progressive aphasia. Neurobiol Aging 35: 2646–2655.

Baggio HC, Sala-Llonch R, Segura B, Marti MJ, Valldeoriola F, Compta Y, et al. 2014. Functional brain networks and cognitive deficits in Parkinson's disease. Hum Brain Mapp 35: 4620–4634.

Blondel VD, Guillaume J-L, Lambiotte R, Lefebvre E. 2008. Fast unfolding of communities in large networks. J Stat Mech Theory E 2008:P10008.

Brier MR, Thomas JB, Fagan AM, Hassenstab J, Holtzman DM, Benzinger TL, et al. 2014. Functional connectivity and graph theory in preclinical Alzheimer's disease. Neurobiol Aging 35:757–768.

Bullmore E, Sporns O. 2009. Complex brain networks: graph theoretical analysis of structural and functional systems. Nat Rev Neurosci 10:186–198.

Calhoun VD. 2004. Group ICA of fMRI toolbox (GIFT). http://icatb.sourceforge.net (accessed May 15, 2016).

Chan MY, Park DC, Savalia NK, Petersen SE, Wig GS. 2014. Decreased segregation of brain systems across the healthy adult lifespan. Proc Natl Acad Sci U S A 111:E4997–E5006.

Chang TY, Huang KL, Ho MY, Ho PS, Chang CH, Liu CH, et al. 2016. Graph theoretical analysis of functional networks and its relationship to cognitive decline in patients with carotid stenosis. J Cereb Blood Flow Metab 36:808–818.

Cox RW. 1996. AFNI: software for analysis and visualization of functional magnetic resonance neuroimages. Comput Biomed Res 29:162–173.

Damoiseaux JS, Rombouts SA, Barkhof F, Scheltens P, Stam CJ, Smith SM, Beckmann CF. 2006. Consistent resting-state networks across healthy subjects. Proc Natl Acad Sci U S A 103:13848–13853.

Di X, Gohel S, Kim EH, Biswal BB. 2013. Task vs. rest-different network configurations between the coactivation and the resting-state brain networks. Front Hum Neurosci 7:493.

Duncan ES, Schmah T, Small SL. 2016. Performance variability as a predictor of response to aphasia treatment. Neurorehabil Neural Repair. DOI: 10.1177/1545968316642522

Falcon MI, Riley JD, Jirsa V, McIntosh AR, Shereen A, Chen EE, Solodkin A. 2015. The virtual brain: modeling biological correlates of recovery after chronic stroke. Front Neurol 6:228

Fischl B. 2012. FreeSurfer. Neuroimage 62:774–781.

Friedman J, Hastie T, Tibshirani R. 2008. Sparse inverse covariance estimation with the graphical lasso. Biostatistics 9:432–441.

Friedman J, Hastie T, Tibshirani R. 2014. glasso: graphical lasso-estimation of Gaussian graphical models. R package version 1. https://cran.r-project.org/web/packages/glasso/index.html (accessed May 15, 2016).

Gamboa OL, Tagliazucchi E, von Wegner F, Jurcoane A, Wahl M, Laufs H, Ziemann U. 2014. Working memory performance of early MS patients correlates inversely with modularity increases in resting state functional connectivity networks. Neuroimage 94:385–395.

Girvan M, Newman ME. 2002. Community structure in social and biological networks. Proc Natl Acad Sci U S A 99: 7821–7826.

Gleichgerrcht E, Kocher M, Nesland T, Rorden C, Fridriksson J, Bonilha L. 2015. Preservation of structural brain network

hubs is associated with less severe post-stroke aphasia. Restor Neurol Neurosci 34:19–28.
Gratton C, Nomura EM, Pérez F, D'Esposito M. 2012. Focal brain lesions to critical locations cause widespread disruption of the modular organization of the brain. J Cogn Neurosci 24:1275–1285.
Hagberg A, Schult D, Swart P, Conway D, Séguin-Charbonneau L, Ellison C, et al. 2004. Networkx. High productivity software for complex networks. https://networkx.github.io/ (accessed May 15, 2016).
Hagberg A, Schult DA, Swart P. 2008. *Exploring Network Structure, Dynamics, and Function Using NetworkX.* Paper presented at the Proceedings of the 7th Python in Science Conferences (SciPy 2008).
Hagmann P, Cammoun L, Gigandet X, Meuli R, Honey CJ, Wedeen VJ, Sporns O. 2008. Mapping the structural core of human cerebral cortex. PLoS Biol 6:e159.
Himberg J, Hyvarinen A, Esposito F. 2004. Validating the independent components of neuroimaging time series via clustering and visualization. Neuroimage 22:1214–1222.
Jirsa V, Sporns O, Breakspear M, Deco G, McIntosh AR. 2010. Towards the virtual brain: network modeling of the intact and the damaged brain. Arch Ital Biol 148:189–205.
Lee J, Fowler R, Rodney D, Cherney L, Small SL. 2010. IMITATE: an intensive computer-based treatment for aphasia based on action observation and imitation. Aphasiology 24:449–465.
Lee MH, Hacker CD, Snyder AZ, Corbetta M, Zhang D, Leuthardt EC, Shimony JS. 2012. Clustering of resting state networks. PLoS One 7:e40370.
Ma Q, Huang B, Wang J, Seger C, Yang W, Li C, et al. 2016. Altered modular organization of intrinsic brain functional networks in patients with Parkinson's disease. Brain Imaging Behav DOI: 10.1007/s11682-016–9524-7.
Milton J, Solodkin A, Hlustik P, Small SL. 2007. The mind of expert motor performance is cool and focused. Neuroimage 35:804–813.
Murray LL. 2012. Attention and other cognitive deficits in aphasia: presence and relation to language and communication measures. Am J Speech Lang Pathol 21:S51–S64.
Muthuraman M, Fleischer V, Kolber P, Luessi F, Zipp F, Groppa S. 2016. Structural brain network characteristics can differentiate CIS from early RRMS. Front Neurosci 10:14.
Newman ME, Girvan M. 2004. Finding and evaluating community structure in networks. Phys Rev E 69:026113.
Onoda K, Yamaguchi S. 2013. Small-worldness and modularity of the resting-state functional brain network decrease with aging. Neurosci Lett 556:104–108.
Rubinov M, Sporns O. 2010. Complex network measures of brain connectivity: uses and interpretations. Neuroimage 52: 1059–1069.
Saffran EM, Berndt RS, Schwartz MF. 1989. The quantitative analysis of agrammatic production: procedure and data. Brain Lang 37:440–479.
Sandberg CW, Bohland JW, Kiran S. 2015. Changes in functional connectivity related to direct training and generalization effects of a word finding treatment in chronic aphasia. Brain Lang 150:103–116.
Smith SM, Jenkinson M, Woolrich MW, Beckmann CF, Behrens TE, Johansen-Berg H, et al. 2004. Advances in functional and structural MR image analysis and implementation as FSL. Neuroimage 23 Suppl 1:S208–S219.
Solodkin A, Hasson U, Siugzdaite R, Schiel M, Chen EE, Kotter R, Small SL. 2010. Virtual brain transplantation (VBT): a method for accurate image registration and parcellation in large cortical stroke. Arch Ital Biol 148:219–241.
Soman S, Prasad G, Hitchner E, Massaband P, Moseley ME, Zhou W, Rosen AC. 2016. Brain structural connectivity distinguishes patients at risk for cognitive decline after carotid interventions. Hum Brain Mapp 37:2185–2194.
Song J, Birn RM, Boly M, Meier TB, Nair VA, Meyerand ME, Prabhakaran V. 2014. Age-related reorganizational changes in modularity and functional connectivity of human brain networks. Brain Connect 4:662–676.
Stevens AA, Tappon SC, Garg A, Fair DA. 2012. Functional brain network modularity captures inter-and intra-individual variation in working memory capacity. PLoS One 7:e30468.
Tinaz S, Lauro P, Hallett M, Horovitz SG. 2016. Deficits in task-set maintenance and execution networks in Parkinson's disease. Brain Struct Funct 221:1413–1425.
Vatansever D, Menon DK, Manktelow AE, Sahakian BJ, Stamatakis EA. 2015. Default mode dynamics for global functional integration. J Neurosci 35:15254–15262.
Ward NS, Brown MM, Thompson AJ, Frackowiak RS. 2003. Neural correlates of motor recovery after stroke: a longitudinal fMRI study. Brain 126:2476–2496.
Warren JE, Crinion JT, Lambon Ralph MA, Wise RJ. 2009. Anterior temporal lobe connectivity correlates with functional outcome after aphasic stroke. Brain 132:3428–3442.
Zachary WW. 1977. An information flow model for conflict and fission in small groups. J Anthropol Res 33:452–473.

Address correspondence to:
E. Susan Duncan
Departments of Cognitive Sciences & Neurology
University of California, Irvine
Room 3130 Biological Sciences III
Irvine, CA 92697

E-mail: duncane@uci.edu